Hapke, J.; Gehrig, F.; Huber, N.; Schulte, K.; Lilleodden, E.T.:
Compressive Failure of UD-CFRP containing void defects:In situ SEM Microanalysis
In: Composites Science and Technology (2011) Elsevier

DOI: 10.1016/j.compscitech.2011.04.009

Compressive Failure of UD-CFRP Containing Void Defects: *In situ* SEM Microanalysis

Julia Hapke[a,*], F. Gehrig[b], N. Huber[a], K. Schulte[b], and E.T. Lilleodden[a]

[a]*Helmholtz-Zentrum Geesthacht, Institue of Materials Research, Materials Mechanics, Geesthacht, Germany*
[b]*TUHH Technical University Hamburg-Harburg, Institute of Polymers and Composites, Hamburg, Germany*

Abstract

Here we present an *in situ* scanning electron microscopy (SEM) investigation of the compressive failure of unidirectional (UD) carbon fibre reinforced polymer (CFRP) composites with varying pre-existing void content. The experiments were carried out within a dual beam microscope, which couples a SEM with a focused ion beam (FIB), allowing sub-surface investigations of damage. In these tests, the specimen is monitored during the entire loading history, allowing the correlation of microstructural changes and the evolving load-displacement behaviour. Therefore, loading characteristics can be linked directly to failure events. Observations of the sequence of events leading to failure showed direct fibre deflection into a kinked shape eventually followed by fibre fracture. Failure of void-containing CFRP was shown to depend on the void shape as well as the proximity of the void to the kink band. In some cases voids stopped the propagation of kink bands, while in other cases the void caused the kink to deflect in a new direction. The failure structure was observed to change with time, both during hold-load segments as well as after unloading. Through cross-sectional ion beam milling in the unloaded state, the sub-surface damage

*Corresponding author
Email address: julia.hapke@hzg.de (Julia Hapke)

was observed and shown to be similar to that observed at the surface.
Keywords: A. Carbon fibres, B. Porosity/Voids, B. Compression, D. Scanning electron microscopy (SEM)

---

1. Introduction

Compressive failure in carbon fibre reinforced polymers (CFRP) has been a focus of research for more than 50 years. Though a general understanding of the failure evolution exists, predictive models are still challenged by the interplay of lots of variables during the failure process. These variables include internal structure as well as the constituents properties, interfacial effects and environmental conditions [1]. One of the major difficulties to this end is the identification of the relevant mechanisms and the sequence of events controlling failure. Furthermore, the majority of test specimens have only been examined *post mortem* until recently. While such analyses can deliver information about the final failure pattern (e.g. deflected fibres into so-called kink bands), no experimental evidence on failure initiation and evolution can be achieved. Such a lack of knowledge greatly limits the development of predictive models. Despite a wide range of currently existing theories about kink band formation in CFRP, there is no description of general acceptance, owing largely to the complexity of compressive testing of composite materials [2, 3]. It is critical to prevent macroscopic buckling and to minimize stress concentrations generated by friction between specimen and gripping. Due to the different load-bearing capacities of its constituents, an inhomogeneous load distribution develops and failure starts at the point of highest stress. Hence, a sophisticated experimental set-up for load introduction is required; the use of dog-bone shaped specimens, as used in metallic materials to specify the failure location, is obviated.

Together with the sudden and catastrophic nature of composite failure, monitoring of early development stages has been one of the major challenges in composite testing for

decades. As a result, most of the currently available models trace back to one of two main and conflicting theories about the process of failure development. One of the first descriptions of composite compressive failure was presented by Rosen [4] in 1965 and is based on the analysis of photoelastic stress patterns by Dow [5]. Rosen treated fibres like columns on an elastic foundation, with each acting individually. While the load is almost entirely carried by the fibres, the matrix only provides lateral support to the fibres. Both fibres and matrix are considered to deform linear elastically. During loading, fibres buckle into a sinusoidal wavelength pattern; depending on fibre volume content the fibres buckle either in- or out-of-phase. In the range of commercially used composites with fibre volume contents well above 50%, in-phase deflection of the fibres (Fig. 1(a)) is envisaged as the predominant deformation mode. Due to the large shear stresses generated by the buckling fibres within the matrix, Rosen considered the matrix shear modulus G_m to be the decisive parameter governing compressive strength together with fibre volume content. While his theory is applicable to many different fibre-matrix combinations, it results in a severe overestimation of compressive strength, mainly attributed to the assumption of linear-elastic material behaviour. Nevertheless, the description of the failure process, where fibre kinking is the final step of microbuckling, has served as a basis for a large number of studies.With respect to the exact sequence of events, assumptions about the necessity of initial fibre fracture [6, 7] or the formation of a damage zone consisting of crushed fibres [8, 9] prior to fibre kinking are the main enhancements here. Other modifications of Rosen's theory include the consideration of initial fibre misalignment and non-linear material behaviour. Still, no consistence between numerical calculations and experimentally observed compressive strength has been achieved.

In contradiction to Rosen's model, an approach was presented by Argon in 1972 [10]. He describes the failure process as a direct deflection of the fibres into a kinked shape, with no preceding microbuckling (Fig. 1(b)). A high sensitivity to initial fibre misalignment is

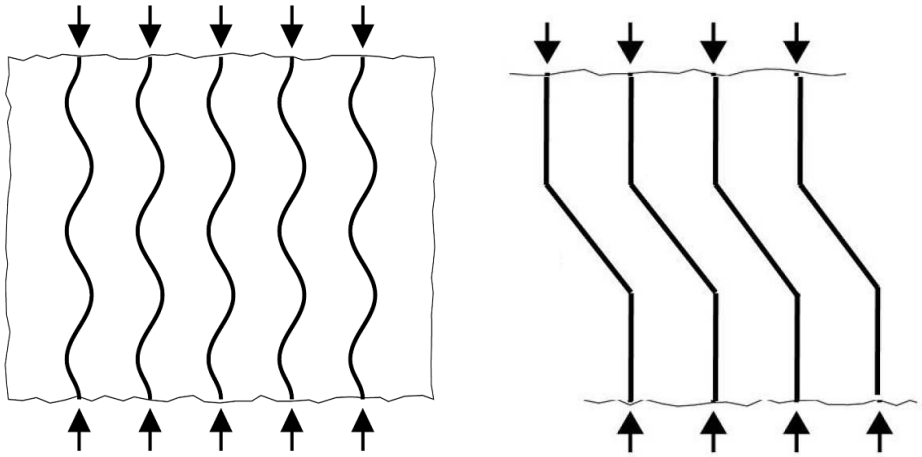

(a) (b)

Figure 1: Schematics of the two major deformation modes proposed for fibre composite materials: In (a), deformation is accommodated by in-phase microbuckling of the fibres as predicted by Rosen [4], (b) shows a direct fibre deflection into a kinked shape according to Argon [10]

attributed to this deformation mode, which is consistent with experimental observations of decreasing compressive strength with increasing misalignment angles. In the matrix, high shear stresses are generated until the matrix shear yield strength is exceeded and visible deformation in the form of kink bands occurs. Due to matrix failure under shear load, these deformation bands are expected to evolve at an angle of roughly 45°. However, Argon's model and its subsequent modifications (e.g. [11–14]) greatly overestimate the compressive strength. Still, it represents the second major fundamental theory about initiation and development of composite compressive failure.

In order to develop a model for reliable and accurate compressive strength prediction, further insight into the governing mechanisms and the sequence of events by advanced experimental methods seems to be necessary. While the prediction of CFRP behaviour under ideal conditions is already challenging, the prediction for CFRP materials containing

flaws and pores is even more so. Such defects are an unavoidable and a critical part of the material behaviour. The fabrication of current composite materials is still a highly manual process [3], with a high risk of introducing unintended fibre misalignment or voids during lay-up and curing. These defects greatly alter the composite's behaviour. As previously described, Argon's model already attempts to include the effect of fibre misalignment on compressive strength, though with a large resultant overestimation. The influence of voids has been subject of numerous studies (e.g. [15, 16]). Voids have been shown to increase fibre misalignment in their vicinity, as well as to change the overall matrix shear behaviour due to variations of the local shear properties.

Given the obvious need for more experimental evidence of the compressive failure mechanisms in CFRP, the study presented here focuses on the experimental identification of the sequence of events prior to and during failure. Monitoring failure on specimens without intentionally introduced or other visible defects, a description of the sequence of events in the ideal state has been determined. In further experiments on void-containing samples, the influence of defects as an additional parameter was analysed. In order to assess the appropriateness of post-mortem investigations and the test method itself, special attention was paid to time-dependent processes during and after testing and to influences of free surfaces on the observed deformation patterns.

2. Experimental

All tests were performed on a unidirectional carbon fibre reinforced epoxy (UD-CFRP), containing 60 % T700 HTS fibres in a 977-2 epoxy resin. Part of the material contains voids introduced by altering the curing cycle, namely by reducing the pressure in the autoclave process from 7 to 2 bar. Small rectangular specimens of 17x5x1 mm were cut from the cured CFRP. A notch was introduced (Fig. 2(a)), acting as a stress riser and thereby minimizing and defining the area where failure is expected to start. It should be mentioned

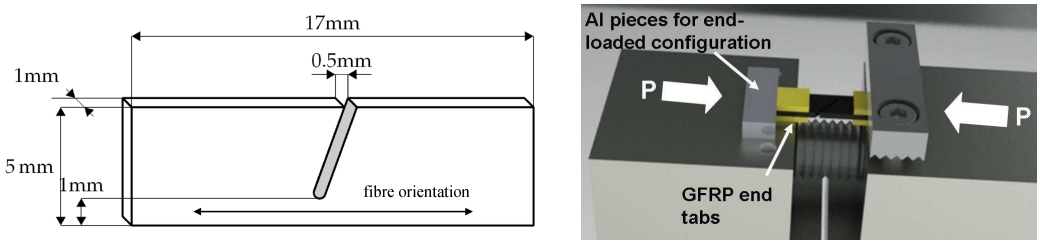

(a) (b)

Figure 2: (a) Final geometry of the test specimens including a notch introduced as stress riser to locate failure area; (b) Loading configuration for testing with pieces of Al used to establish a mainly end-loaded configuration, GFRP-tabs are attached to the specimen's ends to increase the contact area and to reduce friction.

that due to the fact that pre-notching proved to be mandatory to obtain observations of failure initiation with the scanning electron microscope, the stress state at this point becomes non-uniform and only qualitative measurements are possible. Samples were ground with silicon carbide paper and polished using a Al_2O_3-suspension in de-ionised water. After degassing for 24 h at 350 K, a layer of PdAu with a thickness of few nanometers was sputtered on the specimens' surface to improve image quality in the SEM.

For *in situ* mechanical testing, a Gatan 200 microcompression stage was mounted inside a FEI Nova Nanolab 200 dual beam scanning electron (SEM) and focused ion beam (FIB) microscope. The use of the dual beam microscope allows the observation of fibre orientation in layers below the surface and analysis of closely spaced cross-sections in the samples through FIB milling, a technique described in detail elsewhere [17]. A maximum load of 200 N can be applied with the load cell used for all experiments, yielding a load resolution of 2 N. For load introduction, a leading screw is positioned along the loading axis below the sample. The loading direction is parallel to the fibre axis. To avoid failure initiating from stress concentrations caused by load introduction, a mainly end-loaded configuration was chosen and realized using small pieces of aluminum. As shown in (Fig.

2(b)), the Al was placed at both ends of the specimen. Gripping mainly those metal pieces, the load could be transferred to the whole specimen's cross-sectional area while stress concentrations at the surface plies were minimized. For further stress reduction, end tabs made of glass fibre reinforced polymer (GFRP) were attached to the specimens' ends with super glue, yielding a larger area for load introduction and reducing friction between sample and grips. The enlarged contact area between sample and Al-pieces also ensured optimal sample alignment, maintaining a uniform force distribution along the lateral specimen axis to avoid shear loads.

Specimens were loaded parallel to the fibre axis at a constant displacement rate of 0.1 mm/s until first failure was identified. The whole process was captured in a video file at a comparably low resolution, as the quality of SEM images from a moving specimen decreases with increasing magnification. In order to take high-resolution images of better quality, compression was interrupted after first failure and several times thereafter. Loading continued sequentially to further monitor band propagation until a threshold was reached.

Several specimens were examined at different time intervals after the sample was unloaded to gain information about time dependent changes in band morphology. Damage in deeper structures of these specimens was revealed using the focused ion beam (FIB) technique to remove the surface plies. Neither heat nor high mechanical forces are generated during this process [17], which makes this method particularly suitable to avoid preparation artifacts in the analysis of damage in deeper structures. While a small damage layer of a few tens of nanometres in thickness develops due to Ga-bombardment during the FIB milling process, this layer is orders of magnitude smaller than the investigated structures and is therefore not expected to generate artifacts in the analysis.

3. Results and Discussion

The entire deformation process has been observed *in situ* under controlled loading conditions inside the scanning electron microscope. Beginning with tests on specimens without intentionally added defects, the failure process in the ideal state has been determined. The experiment involves observing the development of failure via matrix shearing, kink band formation and fibre fracture, followed by correlating the observations to the load-displacement profile. The results serve as a reference for subsequently tested void-containing specimens. The voids have been located at different positions relative to the evolving kink band in order to analyse orientation-dependent variations. Comparing the results from both types of specimens, the specific influence of voids can be identified.

Further analysis has been performed to identify changes in failure patterns induced by unloading and time-dependent relaxation. The specimens' appearance has been analysed in discrete time steps after the tests, comparable to *post mortem* analysis, in order to observe time-dependent changes in the morphology. To eliminate possible impacts of surface effects on the presented results, the focused ion beam technique has been used to reveal damage occurring in plies below the surface. These deformation patterns were compared to the structures observed at the surface, where effects from specimen preparation and the unsupported free surface might have altered the materials' deformation behaviour.

3.1. Sequence of Events

The first feature visible upon loading is large plastic shearing in the matrix, as evidenced by the formation of shear cups (Fig. 3(a)). Another *in situ* SEM study by Sivashanker et al. [18] on centre-notched specimens revealed fibre kinking as well as longitudinal splitting induced by interfacial debonding. However, such interfacial debonding was not observed in our experiments. Furthermore, the clearly visible matrix degradation shown in Fig. 3(a) supports the assumption of a largely stable fibre-matrix bonding at this

state; it seems that the interface is able to bear much higher loads than the matrix material. However, no statement can be made about possible processes like interfacial sliding, etc., occurring at a smaller scale than is observable here. Fig. 3(a) also reveals bent fibres which are directly deflecting into a kinked shape with no evidence of prior microbuckling. Fibre inclination increases until a kink band starts to propagate, usually located in the most constrained regions close to the notch ground. The video frame in Fig. 3(b) illustrates the sudden and catastrophic nature of band initiation; the visible band has developed within less than 0.2 seconds. At this point (labelled with "110 N" in the loading profile shown in Fig. 4(a)), loading was interrupted for higher resolution imaging. The resultant micrographs of the developed kink band in Fig. 4(b) are taken in the area highlighted in Fig. 3(b) at constant displacement. The images show fibres in a kinked shape ahead of the band tip (Fig. 4(b)). Beyond the fracture zone of the kink band, the length of the inclined fibre segments increases. The final band geometry is defined by fibre fracture, generally advancing at one boundary. Along the band, an increasing out-of-plane deformation toward its initiation site can be observed.

Closer examination of the fibres' fracture surfaces in Fig. 5 reveals smooth lines along the fibre transverse axis on fibres in several plies, suggesting that fracture is mainly driven by the deformation in the thickness direction. As the fibres on the surface plies have been partly removed by sample polishing, this out-of-plane deformation is not necessarily a result of specimen misalignment, but rather a consequence of the surface fibres' reduced load-bearing capacity due to their smaller cross section and damaged internal structure. The issue of possible influences from surface effects will be addressed in greater detail in the section on the analysis of the defect morphology in the plies below the surface. Due to the large out-of-plane deformation, the final fibre inclination and the kink band angle cannot be determined from the SEM images directly. However, bandwidth measurements have been made, showing values in the range of 50 to 60 μm for all bands.

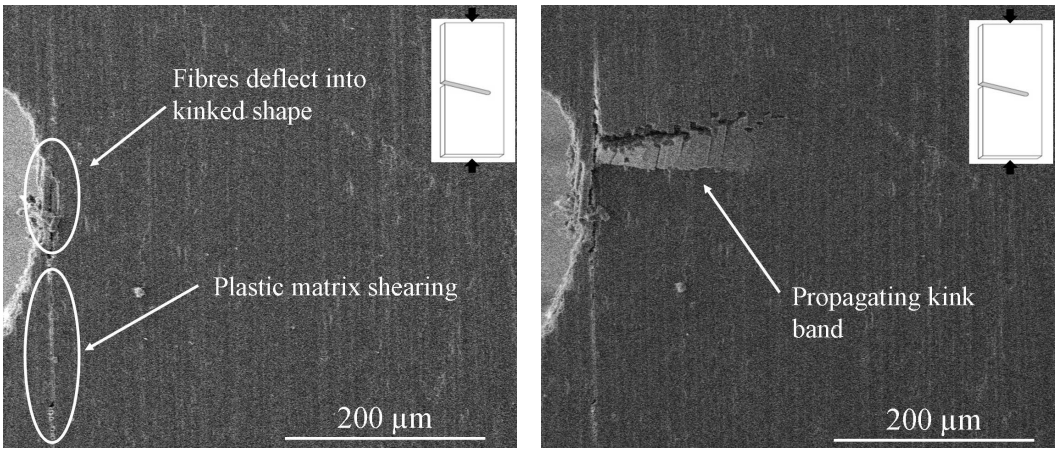

(a) (b)

Figure 3: Two subsequent frames from the movie captured during initial loading. Frame (a) is the last frame before kink band propagation starts. Already visible is large plastic matrix shearing and fibre deflection into a kinked shape. Taken 0.2 sec later, frame (b) shows a kink band already having propagated over more than a 100 μm, illustrating the sudden and catastrophic nature of failure.

As evidenced in Fig. 4(a), every hold segment is accompanied by significant load relaxation. While held at constant displacement before final unloading, further fibre fracture occurred at the band tip, as shown in Fig. 6(a) and 6(b) taken at an interval of 15 minutes during the constant displacement period. During reloading, an additional kink band is initiated at the same site, propagates along the same path and shares one boundary with the original band. The formation of such additional kink bands can be observed on all tested specimens during loading after a holding period. However, only the initial band is ever observed to propagate across the whole width of the sample; subsequent kink bands arrest as soon as the shared boundary with the initial bands terminates.

All events observed during the compression tests resemble what was observed during *in situ* SEM studies by Sutcliffe and Fleck, e.g. [24] as well as the process described by Pimenta et al. [19–23]. In the latter work, *in situ* experiments on CFRP samples

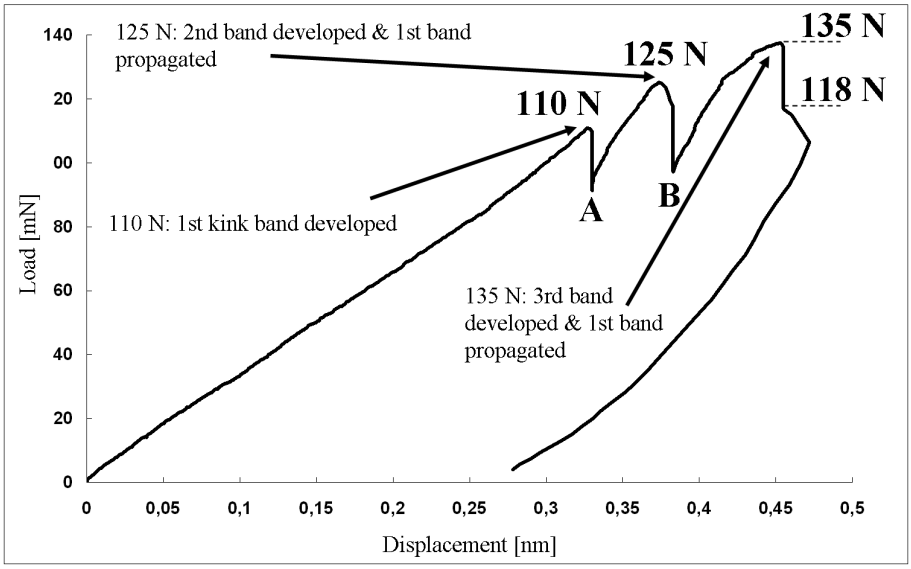

(a)

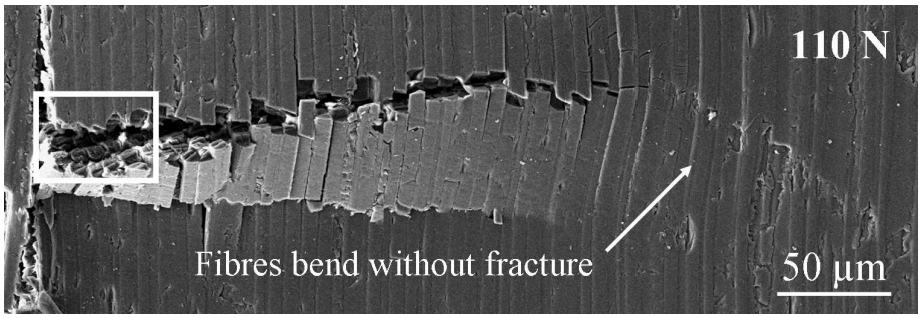

(b)

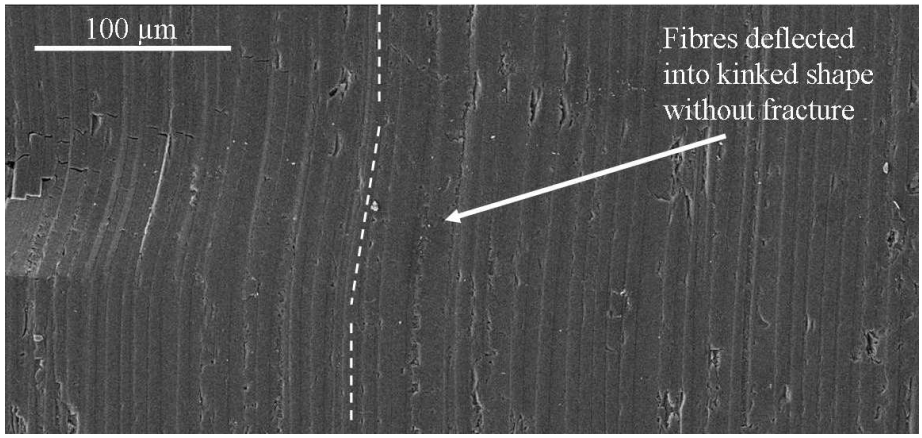

(c)

Figure 4: (a) A generic load-displacement curve including several hold periods for imaging followed by further loading; at the point labelled with 110 N the kink band has been arrested directly after it has started to propagate. The associated images are presented in (b), revealing fibres already bent but not yet fractured ahead of the band tip. Also a large out-of-plane deformation is visible, especially close to the notch ground. In (c), fibre deflection into a kinked shape of yet unfractured fibres is visible in front of the fracture zone.

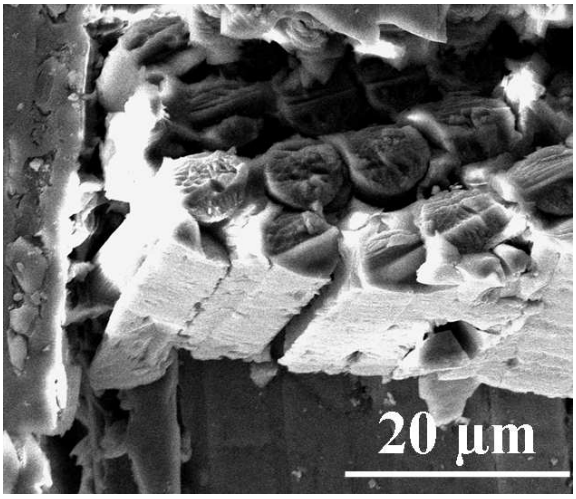

Figure 5: A higher resolution image of the area highlighted in Fig. 4(b), showing lines along the fibre transverse axis on the fibre fracture surfaces, suggesting fracture to be mainly driven by out-of -plane forces.

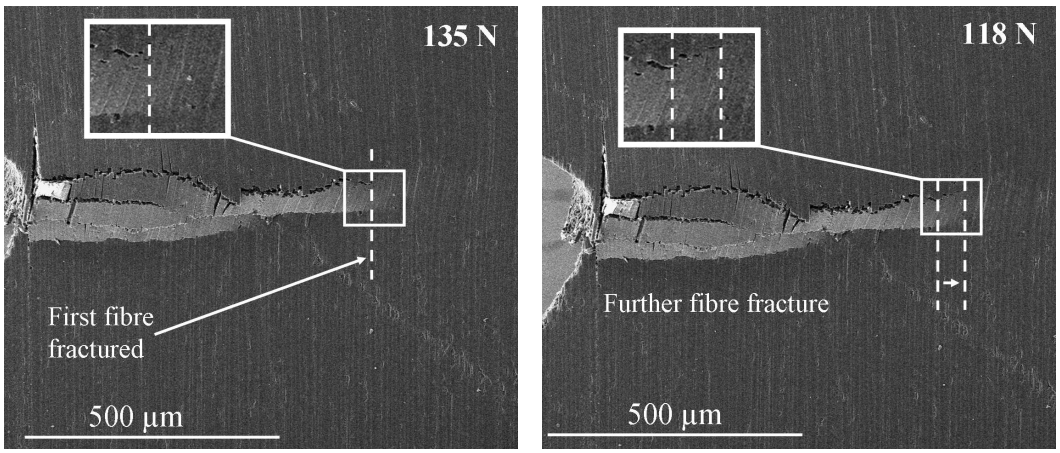

(a) (b)

Figure 6: Images taken at the beginning (a) and 15 min. later at the end (b) of a hold period, marked with 135 N and 118 N in Fig. 4(a). Highlighted areas show further fibre fracture at the band tip, illustrating the large impact of time-dependent processes on damage morphology.

using optical microscopy were combined with numerical and analytical analyses. They conclude that geometric softening of the matrix occurs ahead of the developing kink band. According to their theory, stresses at the band tip increase until the matrix material yields and loses its ability to support the fibres, which are in turn forced to deflect under load. In this context, the additional fibre fracture at constant displacement seems necessary to accommodate the time-dependent behaviour of the polymeric matrix material, resulting in a redistribution of stress from the matrix to the fibres in the highly stressed regions at the band tip. Therefore during reloading it might be energetically more favourable to generate a new kink band in the already softened region close to the stress riser instead of propagating the already existing band. Only if upon further loading the former stress state at the band tip is re-established, the initial band may further propagate.

3.2. Influence of Defects

While the observation of ideal CFRP behaviour under compressive load has been a subject of a few other studies [19–23], no attempts have been made to analyse the behaviour of CFRP structures containing defects. Unfortunately, such defects are present in most materials used in industrial applications. In order to address this reality, defects in the form of voids of similar shape but varying size have been introduced intentionally during the curing process. Under compression, a strong impact on failure evolution was evident in all tested specimens. The overall void content caused a change in the materials behaviour and also the void position relative to the developing kink band was observed to be of importance.

In the case where a kink band propagated along a path in the vicinity of a void tip, a fully developed kink band formed although with a slightly changed shape relative to kink bands in the reference material. This is shown in Fig. 7. With each void passed by the kink band, fibre inclination increases cumulatively, leading to slight changes in the band

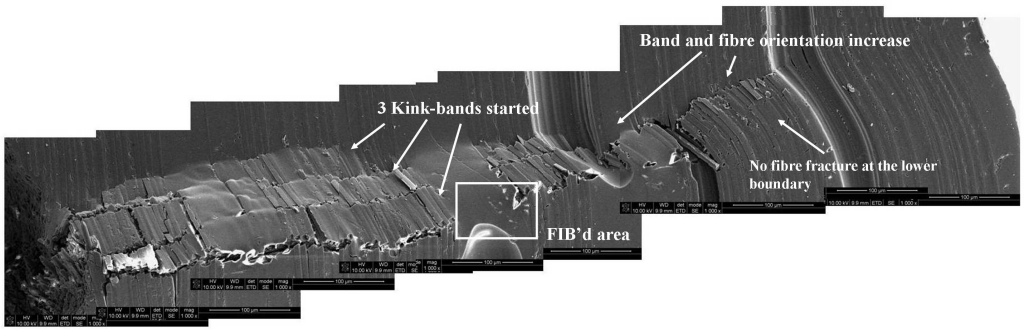

Figure 7: Final kink band morphology in a void-containing specimen. Loading has been interrupted three times, after each hold period a new kink band has started from the stress riser; only one band has propagated over the entire specimen width. Band and fibre inclination increase cumulatively with each void passed; in the final band segment fibre fracture is reduced to only one boundary. In the area highlighted, surface plies have subsequently been removed by the FIB technique to analyse damage morphology in the plies below.

orientation angle. In the segment further away from the stress riser, fibres remain unfractured at the lower band's boundary. All fibres remaining unfractured already deflected into a pronounced kinked shape.

In the case where a defect is located with its centre in front of the defect (Fig. 7), no failure propagation through the void can be observed. Fibres bend and deflect into the void, but the absence of the load-transferring resin seems to effectively hinder band propagation. Resin-rich areas, usually found to circumvent voids in composite materials, were not observed to have any influence on band evolution.

3.3. Time-dependent Behaviour

Two specimens were analysed weeks after testing to examine the effects of time-dependent relaxation. One sample was re-examined two weeks after testing (Fig. 9(a)) and a second one four weeks after testing (Fig. 9(b)). In both cases significant changes in the failure pattern are evident. Fibres and voids have almost completely returned to their original configuration and the fibres' kinked shape has vanished. A *post mortem* investiga-

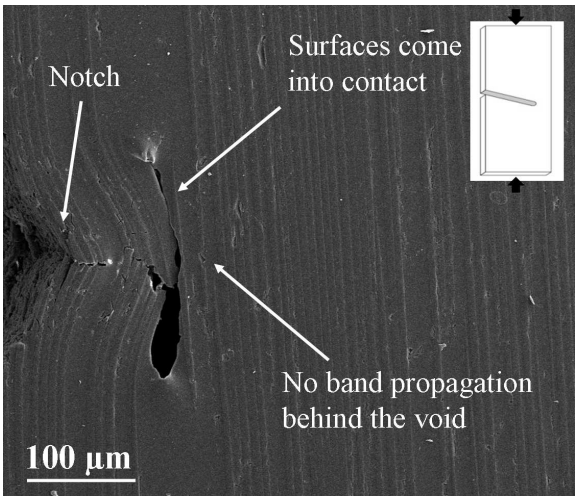

Figure 8: Final kink band morphology in a void-containing specimen; in contrast to the specimen presented in Fig. 7 here the kink band had to propagate directly into the void's centre. Fibres and matrix undergo large deformations bringing the void's inner surfaces into contact, no band propagation behind the void can be observed.

tion in this case would have delivered no meaningful information about the initial failure morphology in terms of band angle, fibre inclination and matrix shearing. The structural changes occurring in the interim between testing and examination would have greatly influenced conclusions made. However, other parameters such as the number of fractured fibres, the fracture path and band width can still be identified in *post mortem* analysis.

3.4. Surface Effects

The focused ion beam (FIB) technique was used to reveal the remaining damage structures below the surface. The main objective was to gain insight into ply deformation and the extent of fibre fracture unaffected from free surfaces and preparation issues. As shown in Fig. 10(a), the fibres' fracture pattern below the surface is identical to that shown at the surface. Even below resin-rich areas broken fibres can be found (Fig. 10(b)), showing the same characteristics as fibres in the band which is visible on the surface. While the CFRP

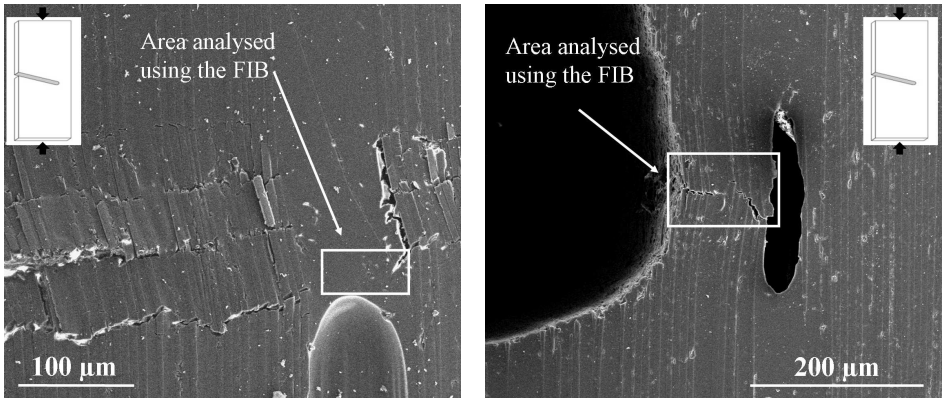

(a) (b)

Figure 9: : In (a), the specimen presented in Fig. 7 is shown two weeks after testing, significant relaxation of the former pronounced kinked fibres is visible. A micrograph of the specimen presented in Fig. 8 four weeks after testing is given in (b); fibres have almost returned into their initial shape. In the areas highlighted in (a) and (b), material has been removed from the surface using the focused ion beam technique.

failure mode is shown to be independent of surface effects, it remains unclear whether failure initiates below the surface or at the surface. Such identification of failure initiation sites will require non-destructive, *in situ* monitoring of the internal structure, as could be realized through *in situ* synchrotron studies.

4. Summary

Compression tests were carried out *in situ* within a SEM on visibly defect-free and void-containing CFRP specimens. The introduction of a stress riser in the form of a notch proved to be mandatory in order to maintain observations of failure development. The sequence of events during compressive failure has been captured in movie files; high-resolution images were taken during frequently introduced holding segments at constant displacement.

Under load, large plastic matrix shearing was visible but no interfacial failure was ap-

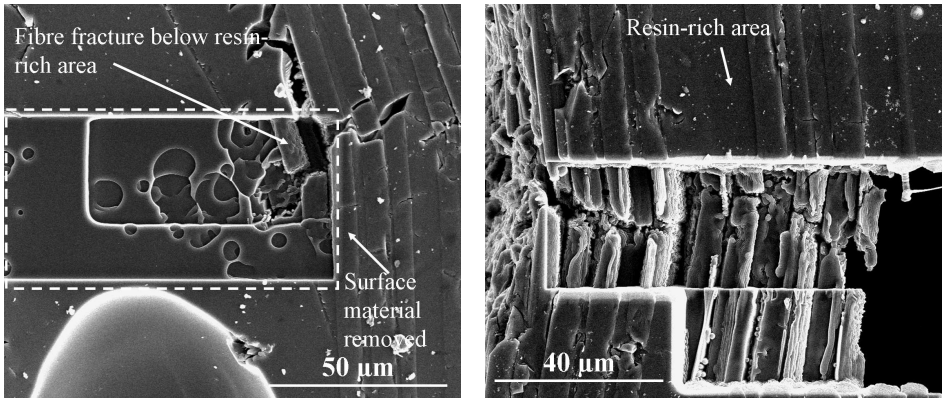

(a) (b)

Figure 10: Fractured fibres below the resin-rich area denoted in Fig. 9(a) can be observed in (a), damage in the sub-surface plies resembling the pattern visible in Fig. 9(b) is presented in (b).

parent. Straight fibres first deflected into a kinked shape and then fractured in a sudden and catastrophic event. However, and in contrast to some proposed models, fibre fracture was not necessary for kink-band initiation and development. Furthermore, neither development of a damage zone consisting of crushed fibres prior to kink band formation nor band broadening has been observed. While observations suggest no decisive role of the interface in the tested materials combination, no statement can be made about possible processes at a smaller scale.

Large out-of-plane deformation was visible in all tested specimens. Closer examination of the fibres' fracture surfaces suggests breakage originating from failure in the thickness direction, most likely directly induced by preparation defects of the surface fibres. Even if the applied load was not increased during constant displacement test segments, further fibre fracture was visible at the band tip. This indicates a decreasing lateral support from the matrix to the fibres due to matrix relaxation. The observations are in good agreement with a currently presented numerical analysis of CFRP compressive failure, suggesting that matrix yielding leads to kinking of the now laterally unsupported fibres.

The bent fibres then create further shear straining of the matrix at the band tip, leading to further fibre deflection and, under certain conditions, to fibre fracture. This process, called geometric softening, is considered to be the main driving force in band evolution. With regard to other theories and models presented so far, it is clearly visible that fibre kinking is not a result of, but rather occurs prior to, fibre fracture.

Voids were found to significantly alter the development of failure. Their influence is not only to be attributed to their shape and density, but also to their position relative to the kink-band. A band propagating in the vicinity of a void tip will change its orientation due to the change in lateral support. In other tests, the kink-band was arrested when propagating into the centre of a void. For both cases, fibre fracture did not occur along the entire band length, though it was always observed with kink band initiation. Further study is necessary to clearly distinguish between the influences of voids and influences of deformation in the thickness direction on fibre fracture.

Analysis of failure morphology within plies below the surface showed patterns consistent with deformation observed at the surface. Hence, no significant changes are to be expected from surface effects in the deformation behaviour, allowing such *in situ* experiments to further the understanding of the failure behaviour of CFRP. Nevertheless, a large influence of time-dependent processes on the band characteristics like fibre inclination, band angle and number of fractured fibres has been observed. The importance of this observation is twofold. It serves as a caution for the interpretation of *post mortem* analysis and indicates that effects of visco-plasticity have to be considered for a more accurate model of CFRP materials' failure.

Acknowledgements

The co-authors F. Gehrig and K. Schulte gratefully acknowledge the support of the Deutsche Forschungsgemeinschaft (DFG) within the project Schu 926/16-1.

[1] Ewins PD, Potter RT Some observations on the nature of fibre reinforced plastics and the implications for structural design. Philosophical transactions of the Royal Society London, 294:507–517, 1980.

[2] Odoms EM, Adams DF Failure modes of unidirectional carbon/epoxy composite compression specimens. Composites, 21:289–296, 1990.

[3] Vogler TJ, Kyriakides S On the initiation and growth of kink bands in fiber composites: Part 1 Experiments. Internal Journal of Solids and Structures, 38:2639–2651, 2001.

[4] Rosen BW Mechanics of composite strengthening. In Fiber Composite Materials, pages 37–73, Metals Park, Ohio, 1964. American Society for Metals.

[5] Dow NF, Gruntfest IJ Determination of most needed potentially possible improvements in materials for ballistic and space vehicles. Technical report, General Electrical Company, Space Science Laboratory, TISR6OSD389, 1960.

[6] Steif PS A model for kinking in fiber composites - 1. Fiber breakage via microbuckling. Internal Journal of Solids and Structures, 26(5/6):549–561, 1990.

[7] Steif PS. A model for kinking in fiber composites - 2. Kink band formation. Internal Journal of Solids and Structures, 26(5/6):563–569, 1990.

[8] Lankford J Compressive failure of fibre-reinforced composites: Buckling, kinking and the role of the interphase. Journal of Materials Science and Technology, 30(17):4343–4348, 1995.

[9] Narayanan S, Schadler LS Mechanisms of kink-band formation in graphite/epoxy composites: A micromechanical experimental study. Composites Science and Technology, 59:2201–2213, 1999.

[10] Argon AS Fracture of Composites:. In Treatise on Materials Science and Technology, 79–114, New York, 1972. Academy Press.

[11] Schultheisz CR, Waas AM Compressive failure of composites, part 1: Testing and micromechanical theories. Progress in Aerospace Science, 32:1–42, 1996.

[12] Vogler TJ, Hsu SY, Kyriakides S On the initiation and growth of kink bands in fiber composites: Part 2 Analysis. Internal Journal of Solids and Structures, 38:2653–2682, 2001.

[13] Ha JB, Nairn JA Compression failure mechanisms of single-ply, unidirectional, carbon-fiber composites. Sampe Quartely, 23(3):29–36, 1992.

[14] Moran PM, Liu XH, Shih CF Kink band formation and band broadening in fiber composites under compressive loading. Acta Metallurgica et Materialia, 43(8):2943–2958, 1995.

[15] Olivier P, Cottu JP, Ferret B Effects of cure cycle pressure and voids on some mechanical properties of carbon/epoxy laminates. Composites, 26(7):509–515, 1995.

[16] Huang H, Talreja R Effects of void geometry on elastic properties of unidirectional fiber reinforced composites. Composites Science and Technology, 65:1964–1981, 2005.

[17] Volkert CA, Minor AM Focused ion beam microscopy and micromachining. MRS Bulletin, 32:389–395, 2007.

[18] Sivashanker S, Osiyemi SO Uniaxial Compressive Failure of Unidirectional Composites with Small Imperfections. Metallurgical and Materials Transactions A, 30A:1867–1876, 1999.

[19] Pimenta S Micromechanics of kink-band formation. Master's thesis, Imperial College London, 2008.

[20] Pimenta S, Gutkin R, Pinho ST, Robinson P A micromechanical model for kink-band formation: Part 1 - Experimental study and numerical modelling. Composites Science and Technology, 69 (Issue 7-8):948–955, June 2009.

[21] Pimenta S, Gutkin R, Pinho ST, Robinson P A micromechanical model for kink-band formation: Part 2 - Analytical modelling. Composites Science and Technology, 69 (Issue 7-8):956–964, June 2009.

[22] Gutkin R, Pinho ST, Robinson P, Curtis PT Micro-mechanical modelling of shear driven fibre compressive failure and of fibre kinking for failure envelope generation in CFRP laminates. Composites Science and Technology, 70:1214,1222, 2010.

[23] Gutkin R, Pinho ST, Robinson P, Curtis PT On the transition from shear-driven fibre compressive failure to fibre kinking in notched CFRP laminates under longitudinal compression. Composites Science and Technology, 70:1223–1231, 2010.

[24] Sutcliffe MPF, Fleck NA Microbuckle Propagation In Carbon Fibre-Epoxy Composites. Acta Metallurgica et Materialia, 42:2219–2231, 1994.